

### Proton-Oxygen Differential Scattering Cross Sections. III\*

G. HARDIE,† R. L. DANGLE, AND L. D. OPPLIGER  
 University of Wisconsin, Madison, Wisconsin  
 (Received 23 July 1962)

A thin gas target (~2.5 keV) was used to measure proton-oxygen elastic scattering cross sections in 2.5-keV steps at  $\theta$ (c.m.) =  $166^{\circ}52'$  for  $8.5 \leq E_p \leq 13.6$  MeV. Similar data were then taken at seven other c.m. angles;  $140^{\circ}46'$ ,  $122^{\circ}35'$ ,  $109^{\circ}53'$ ,  $90^{\circ}00'$ ,  $76^{\circ}12'$ ,  $54^{\circ}44'$ , and  $28^{\circ}08'$  but with energy steps ranging from 5 to 25 keV. Detailed angular distributions of the elastic scattering were taken at roughly 0.5-MeV intervals throughout this energy range, the energies being chosen in order to avoid pronounced resonance structure. In addition, angular distributions were taken at energies of 4.792, 5.870, and 7.009 MeV, in the region previously investigated by Salisbury. All the elastic scattering cross sections are of about 1.5% accuracy.  
 $O^{16}(p, p_i)O^{16*}$  differential cross sections (good to ~10-15%)

for  $p_i = p_1 + p_2$  and  $p_i = p_3 + p_4$  were measured at  $\theta(\text{lab}) = 166^{\circ}00'$  and  $86^{\circ}24'$ . The  $166^{\circ}00'$  inelastic data extend from 10.45 to 12.98 MeV with energy steps identical with the elastic data. The  $86^{\circ}24'$  data for  $p_1 + p_2$  extend from 8.5 to 11.7 MeV, while the  $p_3 + p_4$  group was studied from 9.1 to 11.7 MeV.

The positions and widths of 18 levels in  $F^{17}$  were obtained by inspection of the excitation curves. Two of these levels ( $E_x = 12.522$  and  $13.034$  MeV) had widths of less than 5 keV.

The elastic scattering angular distributions were analyzed using the optical model. Although quite good fits were found for the more forward angles, it was not possible to obtain agreement for  $\theta(\text{c.m.}) > 136^{\circ}00'$ . The extracted optical-model parameters are presented.

#### INTRODUCTION

THIS paper reports an extension of the study of the elastic scattering of protons by oxygen presented in paper II<sup>1</sup> of this series. In the present work the incident laboratory proton energy ranges from 8.5 to 13.6 MeV. Elastic scattering angular distributions at selected energies are also reported. Some inelastic data<sup>2</sup> at laboratory scattering angles of  $166^{\circ}00'$  and  $86^{\circ}24'$  are presented.

#### EXPERIMENTAL PROCEDURE

The equipment and procedures are the same as in II<sup>1</sup> except for the inelastic cross-section data.

A typical pulse-height spectrum obtained with the CsI(Tl) crystal is shown in Fig. 1. Scalers A, B, C, D, E,

and F, with their discriminators set at positions indicated on the figure, were used to sort out the elastic and inelastic yields. The scalar system (A, B, C) determined the yield from the elastic scattering process; scalars D and E determined the yield of inelastic protons  $p_1 + p_2$  corresponding to the first and second excited states of  $O^{16}$ . Likewise scalars F and G give the yield of inelastic protons  $p_3 + p_4$  corresponding to the third and fourth excited states of  $O^{16}$ . Of course, where contributions from background are significant, appropriate subtractions were performed.

A differential elastic scattering cross-section survey was made with incident proton energies in the range 8.5 to 13.6 MeV by taking 2.5-keV steps with targets 2.5-keV thick at a center-of-mass scattering angle of  $166^{\circ}52'$ . Excitation curves of the elastic scattering were also obtained at the c.m. angles of  $28^{\circ}08'$ ,  $54^{\circ}44'$ ,  $76^{\circ}12'$ ,  $90^{\circ}00'$ ,  $109^{\circ}53'$ ,  $122^{\circ}35'$ , and  $140^{\circ}46'$  over the proton energy range 8.5 to 12.7 MeV. The energy steps varied from 5 to 25 keV depending upon the structure of the

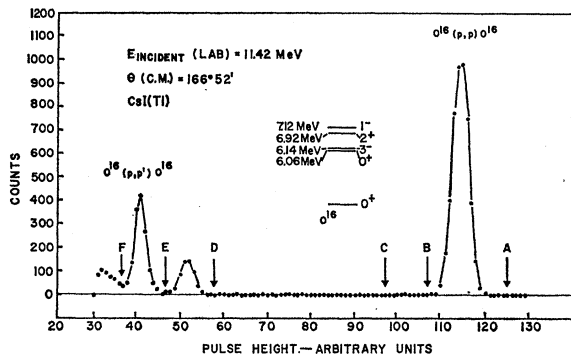


FIG. 1. Elastic and inelastic proton spectrum obtained with the CsI(Tl) detector. The first four excited states of  $O^{16}$  give rise to the two resolved inelastic scattering groups shown.

\* Work supported by the U. S. Atomic Energy Commission and by the Graduate School from funds supplied by the Wisconsin Alumni Research Foundation.

† Now at Armour Research Foundation, Chicago 16, Illinois.  
<sup>1</sup> S. R. Salisbury, G. Hardie, L. Oppliger, and R. Dangle, Phys. Rev. 126, 2143 (1962).

<sup>2</sup> At present a more detailed study of the inelastic data is being conducted at this laboratory and the results will be presented in a later paper.

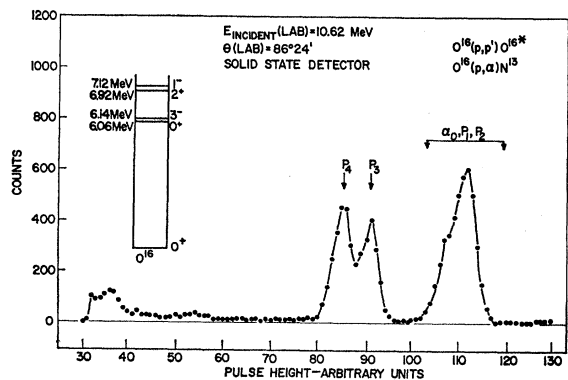


FIG. 2. Spectrum obtained with the  $p-n$  junction detector:  $p_i$  refers to inelastic scattering groups in which the residual nucleus is left in its  $i$ th excited state. The elastic scattering group  $P_0$  is not shown. (Its pulse height is  $> 250$  if bias is sufficient to stop them in the junction.)

survey excitation curve and target thicknesses were always less than 3 keV.

Detailed angular distributions of the elastic scattering were taken at laboratory proton energies usually chosen to miss pronounced resonance structure. The angular spread accepted by the detector slit system was  $\pm 3^\circ$ . The inelastic data at  $86^\circ 24'$  were collected simultaneously with the back angle elastic scattering survey by use of a solid-state detector mounted (with its slit system) on the bottom of the scattering chamber. A spectrum obtained with this detector<sup>3</sup> is given in Fig. 2. The ground-state alpha particles from the reaction  $O^{16}(p,\alpha)N^{13}$  appear under the peak obtained from inelastic scattering leaving the  $O^{16}$  residual nucleus in its first or second excited state. Groups  $p_3$  and  $p_4$  are partially resolved. The resolution was limited by the angu-

lar spread rather than the characteristics of the solid-state detector. (The need to maintain good angular resolution and the requirements imposed on the gas pressure by the elastic scattering work resulted in target thickness of only 0.14 keV for the inelastic data.) For the  $p_1+p_2$  group (which always included the alpha particles) data were taken from 8.5 to 11.3 MeV in 20 keV steps and from 11.3 to 11.7 MeV in 2.5 keV steps. Data for the  $p_3+p_4$  group were taken from 9.1 to 11.3 MeV in 20 keV steps and from 11.3 to 11.7 MeV in 2.5 keV steps.

#### EXPERIMENTAL UNCERTAINTIES

The uncertainties associated with the elastic scattering cross sections are similar to those discussed in paper II.<sup>1</sup> The statistical uncertainties in the yield never ex-

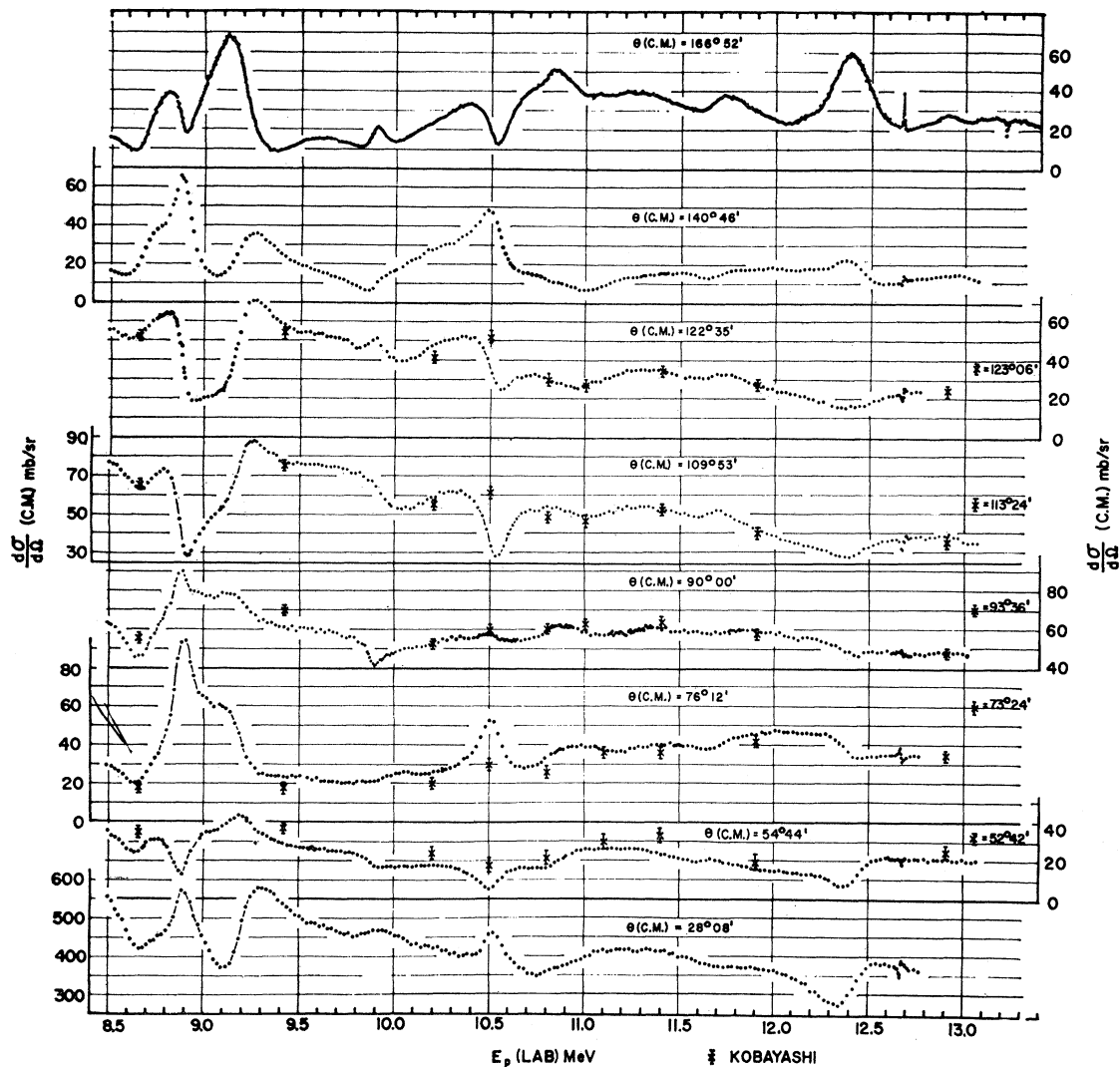


FIG. 3. Elastic scattering excitation curves. Only every third datum point at  $\theta$  (c.m.) =  $166^\circ 52'$  is plotted. Some of Kobayashi's data (see reference 3) are given, his c.m. angles being listed on the right side of each curve.

<sup>3</sup> 5 mm  $\times$  5 mm, 3200  $\Omega$ -cm  $p$ - $n$  junction detector manufactured by Solid State Radiations, Inc., Los Angeles, California.

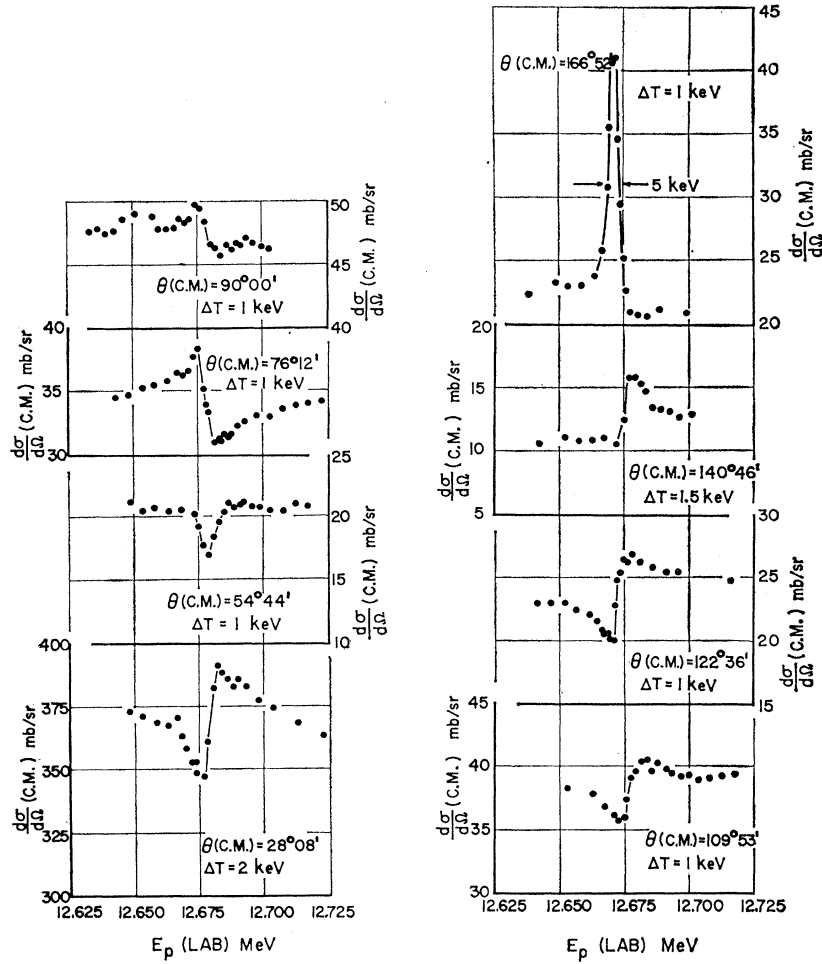


FIG. 4. Details of the sharp resonance at an incident proton energy of 12.67 MeV.  $\Delta T$  is the target thickness.

ceeded 1.3%. Including this uncertainty the rms sum of the uncertainties assigned to each elastic scattering datum point is 1.5%.

By far the largest uncertainties in the inelastic data are associated with the background. For the data at 166°00', the group in which the residual nucleus is left in its third or fourth excited state was assigned an uncertainty, due to the background subtraction, of  $\pm 15\%$ . For the inelastic scattering in which the residual nucleus was left in its first or second excited state the background subtraction uncertainty was estimated to be about  $\pm 15\%$  at the low-energy end (10.5 MeV) and gradually decreasing to about  $\pm 10\%$  at the high-energy end (13.0 MeV).

The inelastic data at 86°24' were not corrected for background, (always less than  $\sim 5\%$ ). Statistical uncertainties were  $\leq 5\%$ .

### EXPERIMENTAL RESULTS

The elastic scattering excitation curves at the various angles are given in Fig. 3. Details of the sharp resonances

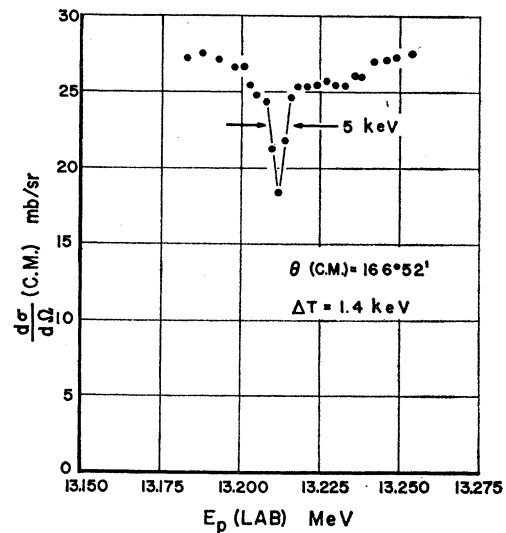


FIG. 5. Details of the sharp resonance at an incident proton energy of 13.2 MeV and at a c.m. angle of 166°52'.  $\Delta T$  is the target thickness.

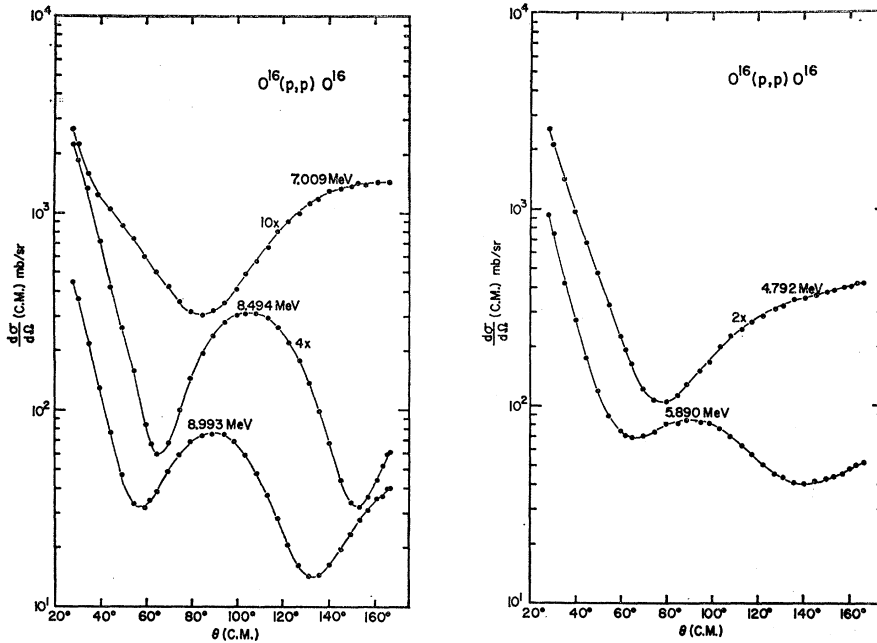


FIG. 6. Angular distributions of the elastic scattering. The energies are incident laboratory proton energies. The cross sections have been multiplied by the indicated values. The lines connect the points in order to make clear the shape of the curves.

observed at 12.67 MeV and at 13.21 MeV are presented in Figs. 4 and 5.

The detailed angular distributions of the elastic scattering are given in Figs. 6 and 7.

Figure 8 presents the inelastic data obtained with the

solid-state detector at  $86^{\circ}24'$ , and with the CsI(Tl) detector at  $166^{\circ}$ . A tracing of the elastic data obtained at the back angle, as well as the data of Whitehead and Foster<sup>4</sup> on the total  $O^{16}(p,\alpha)N^{13}$  cross section, is also presented in this figure for purposes of comparison.

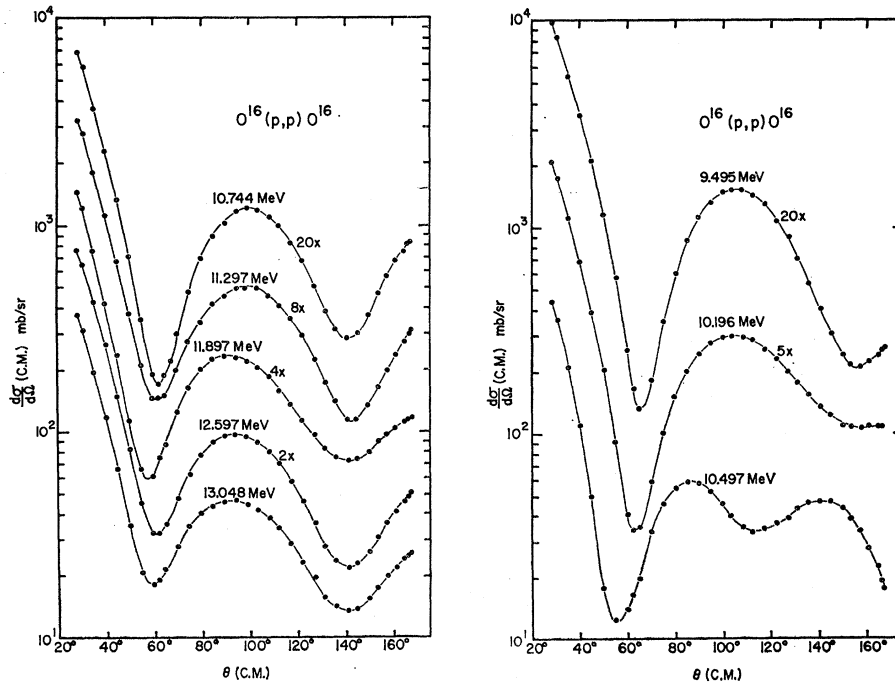


FIG. 7. Angular distributions of the elastic scattering. Also see caption of Fig. 6.

<sup>4</sup>A. B. Whitehead and J. S. Foster, Can. J. Phys. 36, 1276 (1958).

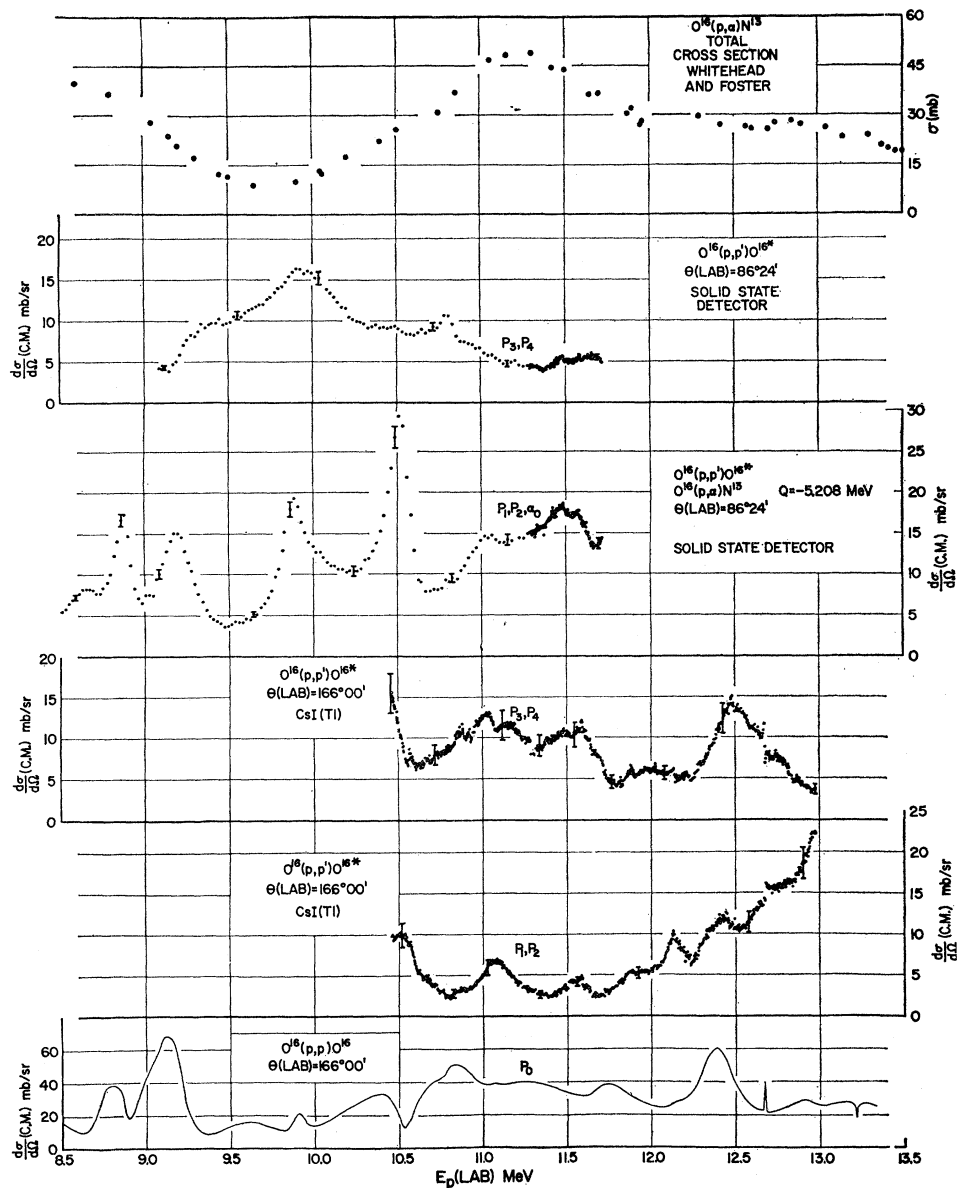


FIG. 8. Inelastic scattering cross sections. The lowest curve is a tracing of the elastic scattering survey at  $\theta$  (lab) =  $166^\circ$ .  $P_i$  refers to inelastically scattered protons which leave the residual nucleus in its  $i$ th excited state. Uncertainties introduced by the background subtraction at  $\theta$  (lab) =  $166^\circ$  are shown on the curve. At  $\theta$  (lab) =  $86^\circ 24'$  the uncertainties shown are statistical.

### DISCUSSION OF RESULTS

Kobayashi<sup>5</sup> studied the elastic scattering of protons by oxygen in an energy region which partially overlaps that of the present data. Some of Kobayashi's results are presented in Fig. 3. Using the angular distributions presented in Figs. 6 and 7 to compensate for the different scattering angles it is seen that agreement is very good. Of course, Kobayashi's energy resolution (several hundred keV) is much poorer than ours and in regions of rapidly varying cross sections Kobayashi's results compare well with the present data averaged over a suitable energy interval.

Inspection of the elastic and inelastic excitation curves

permitted the extraction of approximate resonant energies ( $E_R$ ) and laboratory widths ( $\Gamma$ ) of some of the levels in  $F^{17}$ . This information is given in Table I. Also given in this table are Sturgeon's results<sup>6</sup> obtained by studying the gamma rays from the  $O^{16}(p, p'\gamma)O^{16}$  reaction. The levels extracted from our data are also displayed on Fig. 9 along with some information on the levels of  $N^{17}$ . The position of the ground state of  $N^{17}$ , given with respect to the  $F^{17}$  ground state, was computed from the known masses by taking into account the neutron-hydrogen mass difference and then applying a first-order Coulomb correction.

The two sharp levels, at excitation energies of 12.522

<sup>5</sup> S. Kobayashi, J. Phys. Soc. Japan 15, 164 (1960).

<sup>6</sup> R. F. Sturgeon, M.S. thesis, Florida State University, 1962 (unpublished).

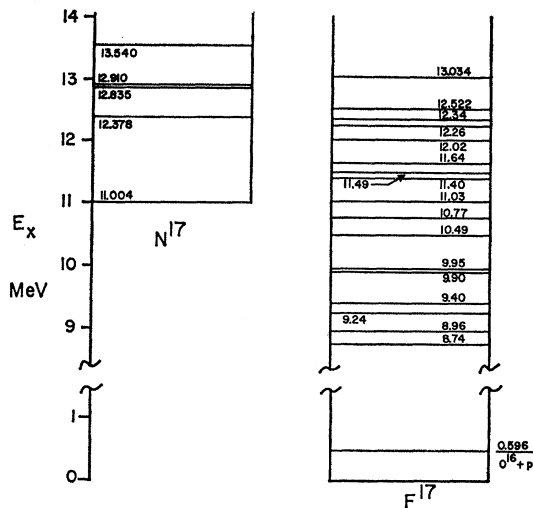


FIG. 9. Comparison of levels in  $N^{17}$  and our  $F^{17}$  levels with ground state of  $N^{17}$  adjusted to  $E_x$  expected for first  $T=3/2$  level of  $F^{17}$  (see text).

and 13.034 MeV, merit special comment. The small widths may be due primarily to centripetal barrier factors if the states have high spin. However, another possibility is that the levels are  $T=3/2$  analogs to the low-lying states in  $N^{17}$ . It is tempting to associate the level at  $E_x=12.522$  MeV with the first excited state of  $N^{17}$ . Similarly the sharp anomaly at  $E_x=13.034$  MeV could be associated with the second or third excited state of  $N^{17}$  which form a close doublet. It is interesting to note on Fig. 5 that there is a suggestion of a doublet structure on the resonance at  $E_p=13.215$  MeV ( $E_x=13.034$  MeV). If the isotopic spin suggestion is correct, then the small widths would be interpreted as arising from the operation of the isotopic spin selection rule. One must still account for the absence of a narrow

TABLE I. Levels in  $F^{17}$ .

$E_p$ (lab) (MeV)	Excitation in $F^{17}$ (MeV)	$\Gamma$ (lab) (keV)
$8.65 \pm 0.05$	8.74	200
$8.88 \pm 0.03$	8.95 (8.935) <sup>a</sup>	$125 \pm 25$ (100) <sup>a</sup>
$9.12 \pm 0.03$	9.18	$225 \pm 30$
$9.18 \pm 0.03$	9.24 (9.24)	$220 \pm 30$ (180)
$9.35 \pm 0.05$	9.40 ( $\approx 9.44$ )	$240 \pm 50$ (300-500)
$9.98 \pm 0.03$	9.90 (9.89)	$130 \pm 50$ (150)
$10.00 \pm 0.03$	10.01 (9.91)	$330 \pm 100$ ( $\approx 300$ )
$10.51 \pm 0.03$	10.49	$125 \pm 25$
$10.81 \pm 0.03$	10.77	$145 \pm 50$
$11.08 \pm 0.03$	11.02	$210 \pm 30$
$11.49 \pm 0.04$	11.41	$190 \pm 70$
$11.57 \pm 0.04$	11.49	$160 \pm 70$
$11.73 \pm 0.05$	11.64	$160 \pm 40$
$12.13 \pm 0.03$	12.01	$200 \pm 50$
$12.39 \pm 0.04$	12.26	$225 \pm 50$
$12.47 \pm 0.05$	12.33	$300 \pm 50$
$12.671 \pm 0.003^b$	12.522	$< 5$
$13.215 \pm 0.004^b$	13.034	$< 5$

<sup>a</sup> Numbers in parentheses are Sturgeon's ( $p, p'\gamma$ ) results, reference 6.

<sup>b</sup> Uncertainty in  $E_p$  does not include the uncertainty in the energy scale as discussed in reference 1.

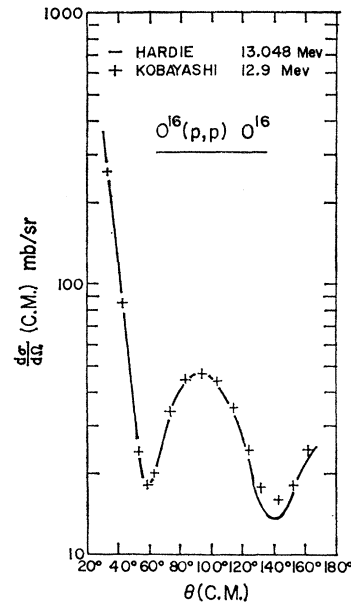


FIG. 10. Comparison of the shape of our experimental curve at 13.048 MeV with Kobayashi's data at 12.9 MeV.

level in  $F^{17}$  near  $E_x \approx 11$  MeV which should correspond to the  $N^{17}$  ground state. The simplest explanation would be to assume that the  $F^{17}$  level has  $\Gamma \ll 2$  keV and hence would be experimentally unobservable. Another possibility is that a neighboring  $T=1/2$  level in  $F^{17}$  exists with the same spin and parity as the  $N^{17}$  ground state

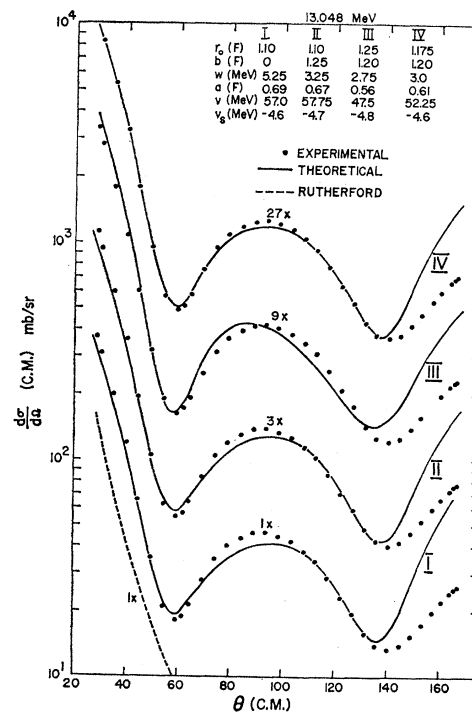
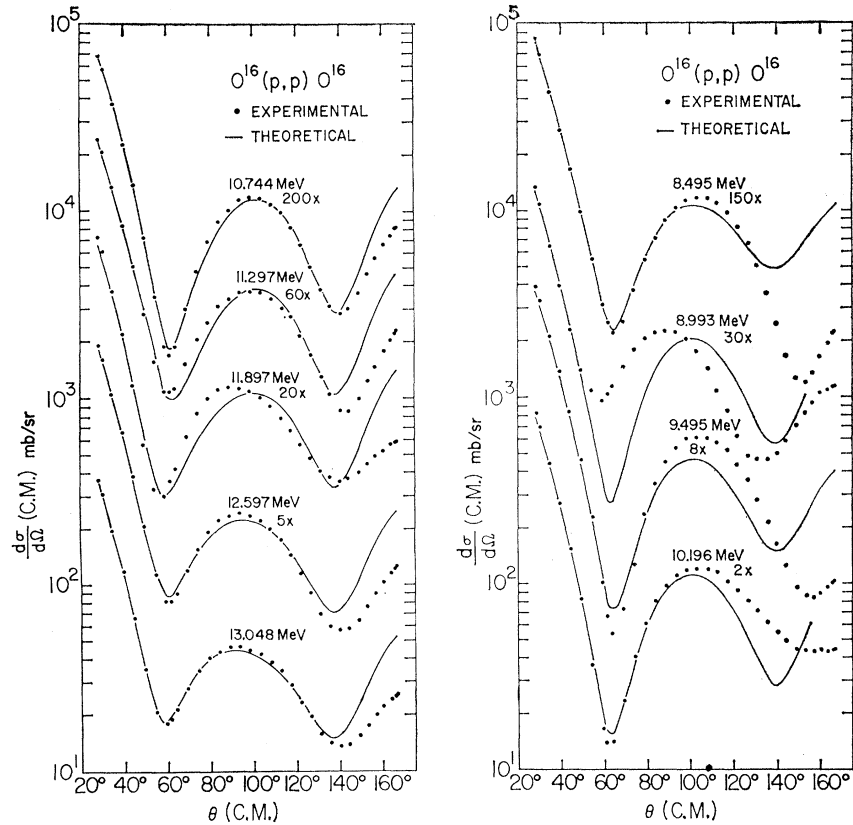


FIG. 11. Various best optical-model fits to the data at 13.048 MeV. Angles greater than  $136^\circ$  were not included in the fits (see text). For clarity the curves have been displaced by the indicated factors.

FIG. 12. Optical-model fits to the angular distributions, see also Fig. 11.



and is appreciably mixed with the  $T=3/2$  analog state by the Coulomb perturbation. In this case the isotopic spin selection rule may be weakened and the  $F^{17}$  analog level to the  $N^{17}$  ground state would be short-lived and hence broad.

The elastic scattering angular distributions were analyzed in terms of an optical-model potential. The UCLA<sup>7</sup> optical-model code was used. The potential was

of the form

$$V_T = \frac{-V}{1 + \exp[(r-R)/a]} - iW \exp\left[-\left(\frac{r-R}{b}\right)^2\right] + V_s \left(\frac{\hbar}{m_\pi c}\right)^2 \frac{1}{r} \frac{d}{dr} \frac{1}{1 + \exp[(r-R)/a]} (\sigma \cdot L) + V_{Coul.}$$

$V_{Coul.}$  was taken to be the electrostatic potential energy of a uniform volume charge density of radius  $R$ .  $R$  was

TABLE II. Optical-model parameters for  $R_0=1.175$  F,  $a=0.61$  F,  $b=1.225$  F,  $V_s=-4.8$  MeV.

$E_p$ (lab) (MeV)	$V$ (MeV)	$W$ (MeV)	$\sigma_R$ (Predicted) (mb)
8.495	50.7	1.0	223
8.993	53.0	1.3	226
9.495	50.5	2.0	324
10.196	52.1	2.3	334
10.744	53.5	2.0	300
11.297	51.6	1.4	227
11.897	53.6	2.15	332 (310) <sup>a</sup>
12.597	51.3	2.9	402 (250) <sup>a</sup>
13.048	52.3	2.95	417 (225) <sup>a</sup>

<sup>a</sup> Experimentally observed reaction cross sections.

<sup>7</sup> M. A. Melkanoff, D. S. Saxon, J. S. Nodvik, and D. G. Cantor, *A Fortran Program for Elastic Scattering Analysis with the Nuclear Optical Model* (University of California Press, Berkeley and Los Angeles, 1961).

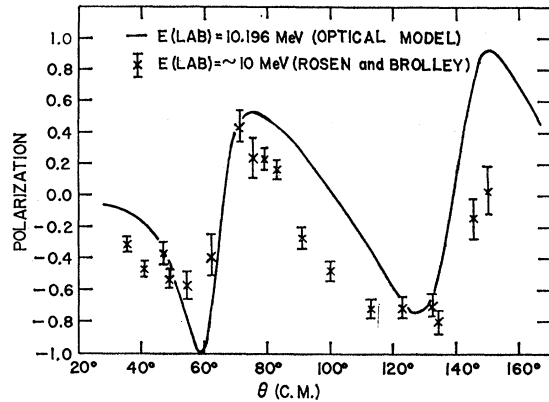


FIG. 13. Comparison of the polarization predicted at 10.196 MeV by our optical-model parameters with the experimental points of Rosen and Brolley at 10 MeV.

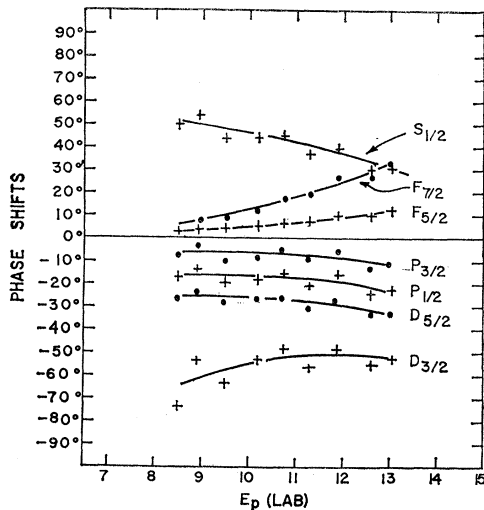


FIG. 14. Real part of the optical-model phase shifts. The optical-model parameters which lead to these phase shifts are presented in Table II.

written as  $R=R_0A^{1/3}$ . The adjustable parameters were  $R_0$ ,  $V$ ,  $W$ ,  $V_s$ ,  $a$ , and  $b$ . In obtaining parameters which would give a best fit to the data, no attempt was made to completely scan the parameter space. Rather a set of parameters considered "reasonable" were taken as a starting set and a local minimum found in the space.

The analysis was started with the angular distribution at 13.048 MeV. Figure 10 gives a comparison of our high resolution angular distribution at 13.048 MeV with Kobayashi's angular distribution at 12.9 MeV. Kobayashi's targets were about 200 keV thick and his beam energy spread was about 0.5%. Hence our angular distribution is very similar to an energy averaged angular distribution, averaging being done over several hundred keV. The back angle data could not be fit by searching the region of parameter space chosen for study. As contributions from isolated resonances will tend to have the greatest effect at the back angle this was not considered a serious limitation. Hence in all subsequent

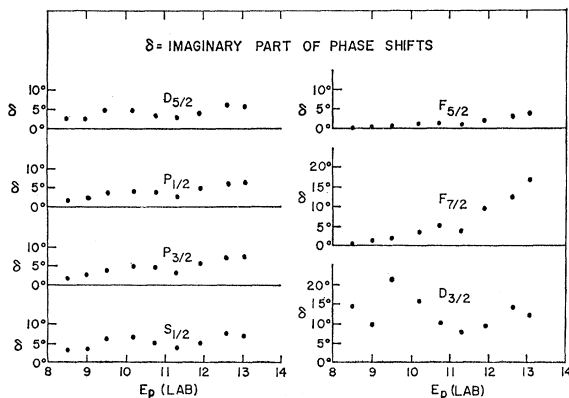


FIG. 15. Imaginary part of the optical-model phase shifts.

fitting work angles greater than  $136^\circ$  in the center-of-mass system were ignored, and in fact the forward angles were more heavily weighted. Figure 11 shows the "best" fits obtained with three choices of the radius parameter  $R_0$ . Of the  $R_0$ 's tried, 1.175 F gives the best fit and this value was employed in all subsequent work.

The other angular distributions were treated in the following manner. All the parameters except  $V$  and  $W$  were kept fixed at the values determined by the fit at 13.048 MeV.  $V$  and  $W$  were varied in order to obtain a "best" fit. As with the work at 13.048 MeV weighting factors were assigned in order to emphasize the more forward angles. The fits are presented in Fig. 12 and the extracted parameters are given in Table II.

The predicted reaction cross sections (which include compound elastic contributions) are also given in Table II, along with the experimentally observed portion of the reaction cross section. This experimentally observed part consists of the  $(p,\alpha)$  channel, as measured by Whitehead and Foster,<sup>4</sup> and inelastic scattering leaving the

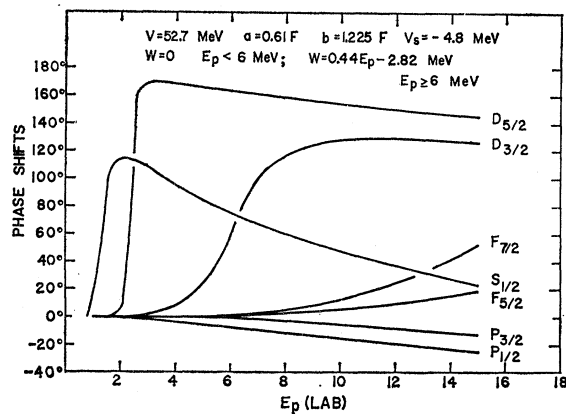


FIG. 16. Phase shifts obtained from a smoothed and extrapolated set of our optical-model parameters.

$O^{16}$  residual nucleus in one of its first four excited states, as measured by Kobayashi.<sup>5</sup> It is unlikely that the other open inelastic channels will contribute appreciably in this energy region. The predicted reaction cross sections seem to be too high at 12.597 and 13.048 MeV. Perhaps compound elastic scattering is responsible for part of the difference.

The polarization predicted by our phase shifts<sup>8</sup> at 10.196 MeV is compared with the data of Rosen and Brolley<sup>9</sup> at 10.0 MeV in Fig. 13.

The extracted real and imaginary phase shifts corresponding to the optical parameters of Table II are presented in Figs. 14 and 15, respectively.

Single-particle resonances are, of course, predicted by a smoothed set of our optical-model parameters. The results are shown in Fig. 16. An  $s_{1/2}$  resonance at about

<sup>8</sup> The predicted polarizations are presented in the Ph.D. thesis of G. Hardie, University of Wisconsin, 1962 (unpublished). Available through University Microfilms, Ann Arbor, Michigan.

<sup>9</sup> L. Rosen and J. E. Brolley, Phys. Rev. **121**, 1423 (1961).



1.4 MeV, a  $d_{5/2}$  resonance at about 2.4 MeV, and a  $d_{3/2}$  resonance at about 6.5 MeV are all clearly evident. The  $f_{7/2}$  phase shift is starting to go through a resonance at the maximum energy. There is no evidence for  $p$  resonances.

The  $d_{5/2}$  and  $s_{1/2}$  resonances presumably correspond to the ground and first excited states of  $F^{17}$ , both of these states having reduced widths which are large fractions of the Wigner limit. A  $d_{3/2}$  single-particle level is experimentally observed at an incident proton energy of 4.67 MeV.<sup>10</sup> It is interesting to note that no prediction

<sup>10</sup> S. R. Salisbury and H. T. Richards, Phys. Rev. **126**, 2147 (1962).

is made of a single-particle  $p_{3/2}$  level similar to the one reported in  $O^{17}$  at an excitation of about 7.7 MeV by Baldinger *et al.*<sup>11</sup>

#### ACKNOWLEDGMENTS

It is a pleasure to thank Professor H. T. Richards for his help and advice on all phases of the project. We wish to thank Professor C. H. Blanchard for many informative discussions on the optical model. We are grateful to R. E. Rothe, D. R. Croley, J. E. Jobst, and F. deForest for aid in collecting the data.

<sup>11</sup> E. Baldinger, P. Huber, and W. G. Proctor, Phys. Acta **25**, 142 (1952).

## Nuclear Resonant Scattering of Gamma Radiation of Variable Energy

W. L. MOUTON, J. P. F. SELLSCHOP, AND G. WIECHERS

*Nuclear Physics Research Unit, University of the Witwatersrand, Johannesburg, South Africa*

(Received 19 February 1962)

A variable-energy gamma-ray system is described. Monoenergetic gamma radiation undergoing Compton scattering produced this energy variability over a significant range. The parameters of the system are described.

Gamma radiation from a  $Co^{60}$  source of strength 1200 C was Compton scattered from a copper scatterer. The energy of the scattered radiation varies continuously from 1.33 MeV in the forward direction to 0.21 MeV at a scattering angle of  $180^\circ$ . The rays of mean energy 480 keV, corresponding to a mean scattering angle of  $69.5^\circ$ , were resonantly scattered by lithium. From a self-absorption experiment the mean life of the first excited state of  $Li^7$  was found to be  $(1.48 \pm 0.35) \times 10^{-13}$  sec.

### I. INTRODUCTION

WHEN inducing nuclear reactions by incident particles, energy variability has proved to be of immense value. In particular, the excitation of only a specific energy level, even when not far removed from neighboring levels, at least facilitates and at times makes possible, the determination of characteristics of the level concerned. For the study of photoreactions there are two main sources of gamma rays. In the first of these a decay from one specific nuclear level to another, gives rise to discrete energy gamma rays. The second source on the other hand is that of electron produced bremsstrahlung with a continuous range of energy values up to a maximum equal to the maximum electron energy. For the excitation of nuclear levels of specific energy, clearly neither source is ideal.

During the past decade gamma radiation has been successfully used for the measurement of widths (and, hence, lifetimes) of both bound and virtual nuclear states. In this period various techniques for nuclear resonant scattering and absorption of gamma radiation have developed rapidly.

In the earliest experiments, high temperature and ultracentrifuge methods were used. Subsequently, resonant scattering has been detected for gamma radiation

which is Doppler broadened in energy as a result of preceding gamma or particle emission.<sup>1</sup> This applies to radiations emitted from both radioactive sources and in nuclear reactions of the type  $(p, p'\gamma)$ . The radiation widths of several bound states in various nuclei have been determined from such measurements. In some elegant experiments the gamma radiation emitted in proton capture reactions has been resonantly absorbed.<sup>2</sup> As a result of the proton capture the subsequent radiation is Doppler shifted in energy. This method is suitable for determining the radiation widths of highly excited states in nuclei. Recently, experiments have been reported in which the source of radiation is bremsstrahlung as produced by accelerated electrons.<sup>3</sup> Since the bremsstrahlung spectrum is continuous, all energy levels can be excited up to the maximum energy of the radiation incident on the scatterer. In this case resonant scattering can be observed provided that the level width is sufficiently large. This method has been used to study both low-energy and highly excited states of nuclei.

<sup>1</sup> C. P. Swann, V. K. Rasmussen, and F. R. Metzger, Phys. Rev. **114**, 862 (1959).

<sup>2</sup> P. B. Smith and P. M. Endt, Phys. Rev. **110**, 397 (1958).

<sup>3</sup> E. C. Booth, Nucl. Phys. **19**, 426 (1960).